Molecular Physics, Vol. 105, Nos. 5–7, 10 March–10 April 2007, 663–677

Taylor & Francis
Taylor & Francis Group

A new potential function form incorporating extended long-range behaviour: application to ground-state Ca_2

ROBERT J. LE ROY*† and ROBERT D. E. HENDERSON†‡
†Department of Chemistry
‡Department of Physics & Astronomy, University of Waterloo,
Waterloo, Ontario N2L 3G1, Canada

(*Received 26 October 2006; in final form 24 January 2007*)

A new analytic potential energy function form which incorporates the two leading inverse-power terms in the long-range potential is introduced and applied to a recently reported data set for the ground $X^1\Sigma_g^+$ state of Ca_2. The new function yields an accurate representation of data which span 99.97% of the well depth and involves only a fraction as many (between 1/3 and 2/3 fewer) parameters as were needed to define published potential functions for these systems based on the same data. Fits using this form also allow a robust determination of the dissociation energy and C_6 dispersion coefficient, and the resulting function is easier to use than other potential functions which have been determined for this system.

1. Introduction

In recent years, interest in the behaviour of ultra-cold atoms has inspired numerous spectroscopic studies of alkali and alkaline earth metal diatomic molecules. Those studies often focused on the determination of accurate potential energy functions for the species of interest, with particular attention being paid to the region very near the dissociation limit. The traditional approach to determining potential energy functions from spectroscopic data consists of two steps: first the data are fitted to analytic expressions for the level energies as functions of the vibrational and rotational quantum numbers v and J; then a pointwise potential energy function is obtained by applying the semiclassical RKR inversion procedure [1] to the resulting analytic expressions for the vibrational energies and inertial rotational constants. That approach has three main shortcomings. First, the first-order semiclassical basis of the conventional RKR procedure means that quantal calculations based on such potentials will not fully reproduce the experimental transition energies they are based on, especially for species of small reduced mass. Second, the pointwise form of the resulting potential functions make them inconvenient to work with, and it introduces 'interpolation noise' uncertainties into quantal calculations using them. Thirdly, unless the parameterized fit to the experimental data is based on near-dissociation expansions [2–7], which is rarely the case, there is no natural way of extrapolating such potentials beyond the region spanned by the data used in the analysis, and one has to rely on an *ad hoc* attachment of analytic extrapolating functions in the short- and long-range regions.

In the last decade and a half, some of the above shortcomings have been addressed by the increasing use of the fully quantum mechanical 'direct-potential-fit' (DPF) method of spectroscopic data analysis. In this approach, observed transition energies are compared to differences between quantum mechanically calculated level energies of a parameterized analytic potential energy function, and a least-squares fit procedure is used to optimize the parameters defining that function. This approach also takes account of Born–Oppenheimer breakdown (BOB) effects through inclusion of atomic-mass-dependent radial strength function contributions to the rotationless and centrifugal potentials, and hence allows a simultaneous unified treatment of data for all isotopologues of the given species. However, a long-standing challenge has been the development of flexible analytic potential function forms which both incorporate the correct theoretically-known limiting long-range behaviour and are 'well-behaved' outside the region spanned by the experimental data used in the analysis. In particular: (i) they should have no spurious extrema or other unphysical behaviour in the interval between the 'data region' centred on the potential minimum and the region near dissociation where the

*Corresponding author. Email: leroy@uwaterloo.ca

Molecular Physics
ISSN 0026–8976 print/ISSN 1362–3028 online © 2007 Taylor & Francis
http://www.tandf.co.uk/journals
DOI: 10.1080/00268970701241656

theoretically-known inverse-power long-range behaviour becomes valid, and (ii) they should approach the imposed limiting behaviour in a physically appropriate manner.

In recent years, a number of different types of potential function models have been introduced and used in successful DPF analyses of data sets which span most of the potential well. However, some of those models require the use of a relatively large number of potential function parameters, and some only take account of the correct long-range behaviour and prevent unphysical short-range behaviour by attaching independent extrapolating functions at the inner and/or outer ends of the data region. The present work presents a new potential energy function model, what we call the 'Morse/Long-Range' or MLR function, which both avoids these problems and incorporates an improved transition between the main potential well and the inverse-power long-range region. Its use is illustrated by its application in an analysis of a very extensive, high quality data set for ground-state Ca_2.

2. Direct potential fits

In a DPF data analysis, the observed rovibrational energy level spacings are fitted directly to differences between eigenvalues of the effective radial Schrödinger equation for the system of interest. For a molecule in a $^1\Sigma$ state, which is the case for the ground electronic state of Ca_2, this effective radial Hamiltonian is most often written in the form proposed by Watson [8, 9],

$$\left\{ -\frac{\hbar^2}{2\mu_\alpha}\frac{\mathrm{d}^2}{\mathrm{d}r^2} + \left[V_{\mathrm{ad}}^{(1)}(r) + \Delta V_{\mathrm{ad}}^{(\alpha)}(r) \right] + \frac{\hbar^2 J(J+1)}{2\mu_\alpha r^2}\left[1 + g^{(\alpha)}(r)\right] \right\} \psi_{v,J}(r) = E_{v,J}\psi_{v,J}(r), \qquad (1)$$

in which $V_{\mathrm{ad}}^{(1)}(r)$ is the total effective adiabatic internuclear potential for a selected reference isotopologue, $\Delta V_{\mathrm{ad}}^{(\alpha)}(r)$ is the *difference* between the effective adiabatic potential for isotopologue α and that for the reference species (labelled $\alpha = 1$), and $g^{(\alpha)}(r)$ is the non-adiabatic centrifugal-potential correction function for isotopologue α. In the application to Ca_2 presented below, the data show no significant dependence on these adiabatic and non-adiabatic BOB terms, so they are not discussed further here (see [10] for a discussion of their forms). This also means that the effective adiabatic potential energy function is the same for all isotopologues of a given species, so the superscript labels '(α)' or '(1)' and the subscript label 'ad' will henceforth be omitted from the symbol for the potential energy function, $V(r)$.

For any given radial potential function, equation (1) may readily be solved by standard numerical methods to yield eigenvalues $E_{v,J}$ and eigenfunctions $\psi_{v,J}(r)$ to virtually any desired accuracy. Differences between appropriate eigenvalues simulate the observed transition energies, while the Helmann–Feynman theorem allows the associated eigenfunctions to be used to generate the derivatives with respect to potential function parameters p_j which are required for performing the least-squares fit to experimental data:

$$\frac{\partial E_{v,J}}{\partial p_j} = \left\langle \psi_{v,J}(r) \left| \frac{\partial V(r)}{\partial p_j} \right| \psi_{v,J}(r) \right\rangle. \qquad (2)$$

In the application discussed in section 4, the quality of fit of an M-parameter model to a set of N experimental data y_i^{obs} with estimated uncertainties u_i is represented by the the dimensionless root-mean-square deviation

$$\overline{dd} \equiv \left\{ \frac{1}{N}\sum_{i=1}^{N}\left[\frac{y_i^{\mathrm{calc}} - y_i^{\mathrm{obs}}}{u_i} \right]^2 \right\}^{1/2}, \qquad (3)$$

where y_i^{calc} is the value of datum i predicted by the model. A 'good' fit is, of course, one which yields a $\overline{dd}$ value close to unity. However, if optimally converged values of $\overline{dd}$ differ somewhat from unity (say $\overline{dd} = 1.44$ or 0.68), it often merely indicates that the estimates of the experimental uncertainties were somewhat too optimistic or too pessimistic, respectively.

The DPF analyses reported in this work were all performed using program DPotFit, which is freely available on the www, together with a comprehensive user manual [11].

3. Model potential functions for DPF analysis

3.1. *General considerations*

A number of detailed DPF data analyses have been based on potential function forms which are generalizations of the simple Morse potential

$$V(r) = \mathfrak{D}_{\mathrm{e}}[1 - \exp[-\phi(r)(r - r_{\mathrm{e}})]]^2, \qquad (4)$$

in which $\mathfrak{D}_{\mathrm{e}}$ is the well depth, r_{e} is the equilibrium internuclear distance and $\phi(r)$ is a (moderately) slowly varying function of r which is represented by some type of polynomial expansion [12–21]. However, potentials of this type die off exponentially at large r, while theory

tells us that at long range, all intermolecular potential functions become a sum of inverse-power terms [22–24],

$$V(r) \simeq \mathfrak{D} - C_n/r^n - C_m/r^m - \cdots, \tag{5}$$

where the values of the integer powers $n < m < \cdots$ etc. characterizing the terms contributing to this sum are determined by the nature of the atoms to which the given molecular state dissociates [22–27], and the associated coefficients, $C_n, C_m, \ldots$ etc., may often be computed from theory. It is reasonable to expect that functions which incorporate this correct limiting long-range behaviour will provide more realistic representations of the potential energy function at distances beyond the data region defined by the inner and outer turning points of the levels involved in the data analysis. Moreover, for cases in which the highest of the observed vibrational levels lie fairly close to the dissociation limit $\mathfrak{D}$, potentials which do not incorporate this type of long-range behaviour will yield an inadequate representation of the experimental data.

In view of the above, it has become increasingly common for DPF data analyses to be based on potential function forms which incorporate the long-range behaviour of equation (5), in one form or another. However, some of those forms have significant shortcomings. For example, some merely attach an inverse-power sum with the form of equation (5) to an independent analytic function determined from a fit to data in the main part of the potential well. As a result, their second- and higher-order (and sometimes also first-order) derivatives are not continuous at the joining point, and this attachment process may introduce a substantial degree of model dependence into attempts to determine dissociation energies or long-range potential coefficients C_n from such analyses. Other forms have what might seem like an excessively large number of fitting parameters, or may depend on *ad hoc* parameters to define the onset of that long-range region. These problems stimulated our development of the potential form discussed below.

3.2. *The Morse/long-range (MLR) potential function*

3.2.1. General. For molecular states in which the observed vibrational levels extend fairly close to the dissociation limit, it is particularly desirable to have a flexible, multi-parameter model potential which naturally incorporates the type of long-range behaviour seen in equation (5). One of the more widely used functions of this type is the 'Morse/Lennard-Jones' or MLJ potential, [28, 29]

$$V_{\mathrm{MLJ}}(r) = \mathfrak{D}_{\mathrm{e}}\left\{1 - \left(\frac{r_{\mathrm{e}}}{r}\right)^n \exp\left[-\phi(r) y_p(r)\right]\right\}^2, \tag{6}$$

where r_{e} is the equilibrium internuclear distance and $\phi(r)$ is a (fairly) slowly varying function of internuclear distance defined such that $\lim_{r\to\infty} \phi(r) = \phi_\infty$ (a finite constant, see below). In the present work, $\phi(r)$ is defined as a constrained power series expansion in the auxiliary radial variable

$$y_p(r) = \frac{r^p - r_{\mathrm{e}}^p}{r^p + r_{\mathrm{e}}^p}, \tag{7}$$

where p is a small positive integer (see below). Since $\lim_{r\to\infty} y_p(r) = 1$, at large r the exponent coefficient $\phi(r)$ approaches the (constant) value ϕ_∞, and equation (6) takes the form

$$V_{\mathrm{MLJ}}(r) \simeq \mathfrak{D}_{\mathrm{e}} - \left\{2\mathfrak{D}_{\mathrm{e}}(r_{\mathrm{e}})^n \exp\left(-\phi_\infty\right)\right\}/r^n = \mathfrak{D}_{\mathrm{e}} - C_n/r^n, \tag{8}$$

where $\phi_\infty \equiv \lim_{r\to\infty} \phi_{\mathrm{MLJ}}(y_p(r)) = \ln\{2\mathfrak{D}_{\mathrm{e}}(r_{\mathrm{e}})^n/C_n\}$, or $C_n = 2\mathfrak{D}_{\mathrm{e}}(r_{\mathrm{e}})^n \exp(-\phi_\infty)$. Thus, the Morse-like potential of equation (6) naturally transforms itself into the limiting single-term inverse-power form of equation (8) for $r \gg r_{\mathrm{e}}$.

The exponent coefficient function $\phi(r) = \phi_{\mathrm{MLJ}}(y_p(r))$ of equation (6) must, of course, be constrained to approach the limiting value (of ϕ_∞) defined by the C_n coefficient as $r \to \infty$. In early work with this model, that behaviour was imposed by using a switching function [28–33], but the same result can be achieved more simply by using a constrained polynomial form in which ϕ_∞ is an explicit parameter [34, 35]:

$$\phi(r) = \phi_{\mathrm{MLJ}}(y_p(r)) = \left[1 - y_p(r)\right] \sum_{i=0}^{N} \phi_i y_p(r)^i + y_p(r)\phi_\infty. \tag{9}$$

As has been shown elsewhere [10, 34–36], use of an exponent expansion of this form based on an expansion variable $y_p(r)$ with $p > 1$ can prevent spurious behaviour both at very short range and in the interval between the data region and the long-range region where the potential takes on the limiting behaviour of equation (8).

The MLJ potential form described above has been successfully used in a number of demanding data analyses [30–33, 35, 37–44]. However, the increasing availability of high-quality data for levels lying very close to the molecular dissociation limit has made it

desirable to have a more sophisticated potential form which can incorporate more than the leading term in the long-range potential of equation (5). This led to our development of what we call the 'Morse/Long-Range' (or MLR) potential

$$V_{\mathrm{MLR}}(r) = \mathfrak{D}_{\mathrm{e}}\left\{1 - \frac{u_{\mathrm{LR}}(r)}{u_{\mathrm{LR}}(r_{\mathrm{e}})}\exp\left[-\phi(r)y_p(r)\right]\right\}^2 \qquad (10)$$

in which the exponent coefficient function $\phi(r) = \phi_{\mathrm{MLR}}(r) = \phi_{\mathrm{MLJ}}(r)$ (see equation (9)) and most other parameters have the same definitions as for the MLJ potential, while $u_{\mathrm{LR}}(r)$ defines the attractive long-range inverse-power behaviour. The MLJ potential corresponds to the simple case in which $u_{\mathrm{LR}}(r) = C_n/r^n$. The present work considers the two-term case in which

$$u_{\mathrm{LR}}(r) = \frac{C_n}{r^n} + \frac{C_m}{r^m} = \frac{C_n}{r^n}\left[1 + \frac{Q_{m,n}}{r^{m-n}}\right], \qquad (11)$$

so that at large r, equation (10) takes the form

$$\begin{aligned} V_{\mathrm{MLR}}(r) &\simeq \mathfrak{D}_{\mathrm{e}} - \left\{\frac{2\mathfrak{D}_{\mathrm{e}}(r_{\mathrm{e}})^n \exp(-\phi_\infty)}{1 + Q_{m,n}/{r_{\mathrm{e}}}^{m-n}}\right\}\left[1 + \frac{Q_{m,n}}{r^{m-n}}\right]\frac{1}{r^n} \\ &\simeq \mathfrak{D}_{\mathrm{e}} - \frac{C_n}{r^n} - \frac{C_m}{r^m}, \end{aligned} \qquad (12)$$

where $C_n = 2\mathfrak{D}_{\mathrm{e}}(r_{\mathrm{e}})^n \exp(-\phi_\infty^{\mathrm{MLR}})/\left[1 + Q_{m,n}/{r_{\mathrm{e}}}^{m-n}\right]$, the quotient $Q_{m,n} = C_m/C_n$ and

$$\begin{aligned} \phi_\infty = \phi_\infty^{\mathrm{MLR}} &= \ln\left\{2\mathfrak{D}_{\mathrm{e}}/u_{\mathrm{LR}}(r_{\mathrm{e}})\right\} \\ &= \ln\left\{2\mathfrak{D}_{\mathrm{e}}(r_{\mathrm{e}})^n/\left[C_n\left(1 + Q_{m,n}/{r_{\mathrm{e}}}^{m-n}\right)\right]\right\}. \end{aligned} \qquad (13)$$

It is clear that equations (10) and (12) collapse to equations (6) and (8) if the factor $Q_{m,n} = 0$, so the MLJ potential is just a special case of an MLR potential. However, it is convenient to use distinct names to distinguish between cases in which two, rather than one, long-range inverse-power terms are incorporated into the potential form.

Finally, in order to ensure that the C_m/r^m term in equation (11) is indeed the second-longest-range term contributing to the potential function, it is necessary to take account of the limiting long-range behaviour of the exponential term in equation (10). At very large r

$$\begin{aligned} &\exp\left[-\phi_{\mathrm{MLR}}(r)y_p(r)\right] \\ &\quad\simeq \exp\left\{-\phi_\infty + 2\left(2\phi_\infty - \sum_{i=0}^{N}\phi_i\right)\left(\frac{r_{\mathrm{e}}}{r}\right)^p\right\} \\ &\quad\simeq \exp(-\phi_\infty)\left(1 + \frac{Q^{\mathrm{eff}}_{n+p,n}}{r^p} + \cdots\right) \end{aligned} \qquad (14)$$

in which $Q^{\mathrm{eff}}_{n+p,n} = 2(2\phi_\infty - \sum_{i=0}^{N}\phi_i)(r_{\mathrm{e}})^p$ and $C_nQ^{\mathrm{eff}}_{n+p,n}/r^{n+p}$ is the leading term contributing to the long-range tail of $V_{\mathrm{MLR}}(r)$ which is not explicitly included in $u_{\mathrm{LR}}(r)$. Thus, it is only when $p > (m-n)$ that the term C_m/r^m in equation (11) actually defines the leading deviations from the limiting $-C_n/r^n$ behaviour. It is clear, therefore, that when using the two-term MLR potential form of equations (10) and (11), the power p defining the exponent radial variable must be greater than the *difference* between the powers of the first and second terms in the long-range potential of equation (5) or (12).

At this point, it might seem intuitively obvious that one should always choose p such that $(n+p) = m_{next}$, the power of the first inverse-power term *not* explicitly included in $u_{\mathrm{LR}}(r)$ which theory predicts should contribute to the long-range intermolecular potential for the state of interest. However, the full long-range potential will also include higher-order terms corresponding to inverse-powers $\geq m_{next}$ [22–25], and virtually all of these long-range terms require damping as r decreases [45–49]. Thus, it may be more reasonable to allow $p \geq (m_{next} - n)$, and have this term represent the *effective* overall leading correction to $u_{\mathrm{LR}}(r)$. This would, perhaps, be the appropriate situation for a system such as Ca_2 where the overall interaction potential is relatively strong.

An alternative to the above scenario might be the case of a very shallow van der Waals potential energy well, for which the repulsive exchange energy becomes important at relatively large distances, and the effective leading correction to $u_{\mathrm{LR}}(r)$ might be negative (repulsive). In this case we would have no expectations regarding the choice of p, other than requiring that $p > (m-n)$. In any case, the full implications of equation (14), and wisdom regarding the choice of p, will only become apparent with further experience. However, the authors would like to state their strong preference for restricting p to integer values. This preference is based partly on the integer nature of powers associated with terms in the long-range potential predicted by theory [22–25] and partly on our very strong preference for simplicity of the analytic form.

3.2.2. Role and significance of the expansion variable. As was mentioned earlier, giving p an integer value greater than 1 (say, $p = 3 - 5$) greatly reduces the probability that a function defined as an expansion in $y_p(r)$ will exhibit non-physical behaviour at distances outside the radial interval to which the data are sensitive [10, 34–36]. The reason for this is made clear by consideration of the plots of $y_p(r)$ for a number of p values shown in figure 1. The interval spanned by the turning points of the levels of ground-state Ca_2 involved

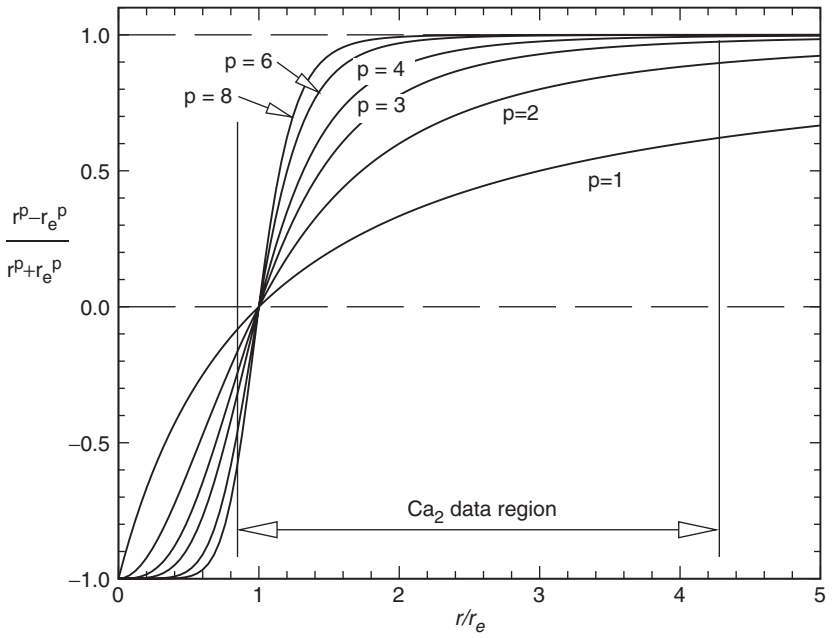

Figure 1. Plot of the expansion variable $y_p(r)$ for various integer values of p, showing the data region for ground-state Ca_2.

in the present data analysis, hereafter referred to as the 'data region', is indicated there. It is immediately clear that for $p = 1$, less than half of the full range of $y_p(r)$ (which is $[-1, +1]$) is spanned by the Ca_2 data region. Thus, it would be unreasonable to expect that a polynomial in $y_1(r)$ determined from a fit to the data would necessarily be 'well behaved' (i.e. have no spurious behaviour) at small and/or large r outside the data region.

The plots in figure 1 clearly show that use of moderately large values of p will strongly inhibit irregular behaviour of functions of $y_p(r)$ outside the data region, since when the expansion variable becomes constant, so does any function defined in terms of it. At the same time, for small values of $|r - r_e|$, $y_p(r) \propto (r - r_e)$ for *all* values of p, so the nonlinear mapping between r and $y_p(r)$ will not inhibit the ability of the latter to provide accurate representations of functions of r in the region near r_e. On the other hand, the fact that $y_p(r)$ plots becomes increasingly flat in the outer part of the data region with increasing values of p means that for those cases, polynomials in $y_p(r)$ will become increasingly less able to provide flexible representations of functions of r at large $|r - r_e|$. In practice this means that for the larger values of p, ever higher-order polynomials in $y_p(r)$ will be required to yield an accurate representation of a given function, and that at sufficiently high p, no plausible increase in the polynomial order will suffice. Illustrations of these considerations are seen in the results presented below.

3.2.3. Inner and outer power-series orders. While use of moderately large values of p to define the expansion variable can usually prevent extrapolation problems at large distances, it does not always simultaneously prevent such problems at small r [36]. This should not be surprising, since a typical diatomic potential well is highly asymmetric, so the polynomial required to accurately describe the behaviour of $\phi(r)$ in the relatively narrow portion of the data region with $r \leq r_e$ would in general be of much lower order than that required for $r > r_e$ (see figure 1). Thus, it seems reasonable to allow the power series expansion of equation (9) to have different orders in these two regions:

$$\phi_{\mathrm{MLR}}(r) = \big[1 - y_p(r)\big] \sum_{i=0}^{N_S} \phi_i y_p(r)^i + y_p(r)\phi_\infty, \quad \text{for } r \leq r_e, \tag{15}$$

$$\phi_{\mathrm{MLR}}(r) = \big[1 - y_p(r)\big] \sum_{i=0}^{N_L} \phi_i y_p(r)^i + y_p(r)\phi_\infty, \quad \text{for } r > r_e. \tag{16}$$

This means that the higher-order terms will not have to compete with one another in the upper part of the inner wall region where they are not really required to define the shape of $\phi(r)$. Of course the coefficients ϕ_i for terms corresponding to powers $i \leq \min\{N_S, N_L\}$ will be the same in both regions, so the only non-analytic behaviour

will be a small discontinuity in derivatives of order $\min\{N_S, N_L\} + 2$ or greater at the one point $r = r_e$.

In the application presented below, particular MLJ or MLR potentials are identified by the value of p defining the expansion variable $y_p(r)$, and by the orders N_S and N_L of the polynomials appearing in equations (15) and (16). For models with $N_S = N_L$ only a single argument will be used, as in $\mathrm{MLJ}_p(N)$, while if $N_S \neq N_L$ the label for the potential model has both orders as arguments, as in $\mathrm{MLR}_p(N_S, N_L)$.

The DPF fitting procedure is highly nonlinear, so one needs to have a realistic set of initial trial potential function parameters to initiate the fit. Such trial parameters may be generated from a fit of the chosen potential form to a mesh of approximate potential function points generated either by *ab initio* calculations or by applying the Rydberg–Klein–Rees inversion procedure [1] to polynomial level energy expressions determined from a Dunham-type analysis [50]. A program for performing fits of this type may be obtained freely (with a user manual) from the first author's www site [51].

4. Application to the ground $X^1\Sigma_g^+$ state of Ca_2

4.1. *Background*

In recent work, Allard *et al*. [52, 53] reported remarkable measurements of 3553 fluorescence series transitions from 180 levels of the $B^1\Sigma_u^+$ state into 924 levels of the ground state of Ca_2. With rotational sublevels extending up to $J'' = 164$, these data spanned the vibrational level range $v = 0$–38, the top of which lies only *ca*. $0.3\,\mathrm{cm}^{-1}$ from dissociation. Since Ca is a closed-shell atom and the available spectra involve only the predominant (96.94% abundance) isotope which has a nuclear spin of zero, this species is an ideal test case for the utility of our new potential function form, since there are no interstate couplings which could affect levels lying very near dissociation.

The analyses of Allard *et al*. [52, 53] were based on direct fits to two different types of models for the potential energy function. In one of these, the potential was based on a polynomial of order 20 (with 21 fitted coefficients) in the effective radial variable $(r - r_m)/(r + br_m)$, where r_m is a fixed distance chosen to lie near the potential minimum and b is a parameter optimized in the fit. Since this form does not extrapolate reasonably at either short or long distances, they also found it necessary to choose inner and outer boundary points R_{inn} and R_{out} at which physically reasonable analytic functions are attached to this polynomial. In the inner region $r \leq R_{inn}$ the function appended was $A + B/r^{12}$, with the values of A and B being defined by the requirement that there be a smooth connection to the high-order polynomial at $r = R_{inn}$; this introduced no additional free parameters to the fit. However, the function attached at R_{out} was the three-term inverse-power expansion

$$V_{out}(r) = \mathfrak{D}_e - C_6/r^6 - C_8/r^8 - C_{10}/r^{10} \qquad (17)$$

in which parameters $\mathfrak{D}_e$ and C_{10} were defined by requiring that $V_{out}(r)$ join the polynomial smoothly at R_{out}, while C_6 and C_8 were free fitting parameters. Thus, this potential function is defined by a total of 24 fitting parameters plus the two selected distances R_{inn} and R_{out}, and derivatives of order two and higher are not continuous at R_{inn} and R_{out}.

The second type of potential function used in the analyses of Allard *et al*. [52, 53] was the 'spline/pointwise' (SPW) form which was originally introduced by Tiemann and co-workers [54–58], and later developed into a generally practical form by Pashov and his collaborators [59–61]. In the SPW approach, the potential function is defined by a cubic spline function passing through a chosen set of grid points, and the energies at those grid points are the parameters to be determined from the fit to the data. For Ca_2 the chosen grid of 48 points included 6 points on the repulsive wall above the dissociation limit, which were defined by an unspecified extrapolation from the well region [53]. Moreover, at distances beyond a chosen value $r = R_{out} = 9.44\,\text{Å}$, the potential was again defined by equation (17), in this case with $\mathfrak{D}_e$, C_6 and C_8 being free fitting parameters and C_{10} being chosen '... to best fit the shape of the pointwise potential between 9.4 and 10 Å'. Thus, for the 48-point grid of [53], this potential has either 45 or 51 free fitting parameters, depending on whether the repulsive wall grid points lying above dissociation are taken as free or fixed, and the degree of analytic continuity at R_{out} is not clear.

Rather than fit the fluorescence series data directly, the analyses of Allard *et al*. [53] replaced them by 8500 ground-state level-energy differences. For the two models described above, the fits yielded average dimensionless deviations of $\overline{dd} = 0.69$ and 0.74, respectively, while the deviations for transitions involving the levels for which $v'' \geq 35$ yielded $\overline{dd} = 0.92$ and 0.89, respectively.

4.2. *Results*

The present analysis is based on the data set reported by Allard *et al*. [53], except that rather than take differences, the 3553 observed transition energies were treated directly, with the 180 fluorescence series origins being treated as free parameters in

Table 1. Dimensionless RMS deviations $\overline{dd}$ for direct fits of various MLJ_p and MLR_p potential forms to the data for ground-state Ca_2.

$N_S; N_L =$	4; 5	4; 6	4; 7	4; 8	4; 9	4; 10	4; 11	4; 12
MLJ_p potentials with C_6 determined by the fit								
$p=2$	0.9598	0.6368	0.6367	0.6341	[a]	[a]	[a]	[a]
$p=3$	1.0614	0.6997	0.6391	0.6352	0.6350	0.6348	0.6346	0.6336
$p=4$	1.7994	0.7653	0.6373	0.6361	0.6359	0.6353	0.6346	0.6345
MLR_p potentials with C_6 fitted while fixing $Q_{8,6} = Q_{8,6}^{\text{theory}} = 30\,\text{Å}^2$								
$p=3$	1.1297	0.7212	0.6409	0.6347	0.6347	0.6346	0.6345	0.6336
$p=4$	1.0412	0.7105	0.7093	0.6777	0.6531	0.6421	0.6359	0.6341
$p=5$	6.3933	3.1689	1.7656	0.9840	0.7128	0.6466	0.6370	0.6356
$p=6$					2.5204	1.7072	1.2380	0.09476

[a]The surfeit of free parameters makes these fits difficult to converge, and causes the fitted C_6 values to have very large uncertainties.

our fits†. All data were weighted by the inverse square of the estimated experimental uncertainties, which ranged from 0.004 to 0.032 cm^{-1}. The difference between the number of transitions used herein (3553) and the number of assigned transitions mentioned in [53] (3580) reflects the omission of a handful of blended or very weak lines which had much larger uncertainties†.

Since ground-state Ca_2 dissociates to two ^1S state atoms, the powers of the two leading terms in the long-range inverse-power potential are $n=6$ and $m=8$ [26, 27], and good estimates of the associated coefficients are available from theory [62–64]. In particular, Moszynski *et al.* [64] recently reported an accurate relativistic value of $C_6 = 1.0366 \times 10^7\,\text{cm}^{-1}\,\text{Å}^6$, while in slightly earlier work, Bussery-Honvault *et al.* [63] reported C_6 and C_8 coefficients which yield the factor $Q_{8,6} = C_8/C_6 = 30\,\text{Å}^2$, for which the estimated uncertainty is ±10% [65]. However, since the experimental data include a number of levels lying very near dissociation, with the outer turning point of the highest observed vibrational level ($v'' = 38$) lying beyond 18 Å, it should be possible to determine an accurate value of at least the leading coefficient from the experimental data. As a result, the coefficient C_6 was treated as a free parameter in most of the fits reported below, while unless stated otherwise, $Q_{8,6}$ was held fixed at the theoretical value of $30\,\text{Å}^2$.

Table 1 lists the dimensionless RMS deviations for fits of the Ca_2 data to MLJ_p and MLR_p potentials for a range of p values and a variety of orders for the exponent polynomial in equations (15) and (16). Prelimnary fits show both that $N_S = 4$ was sufficient to describe the inner wall accurately, and that further increasing or decreasing this value caused many of the resulting potentials either to turn over at small r, or to yield a lower quality of fit. None of the $N_S=4$ cases exhibit turnover or other spurious behaviour at small r, so $N_S=4$ was used for all the potential models discussed below.

As would be expected, for a given potential form and value of p, the quality of fit improves as the order of the exponent polynomial increases. However, it is noteworthy that for all cases, as N_L increases the values of $\overline{dd}$ drop to a common plateau, and are not significantly affected by further increases in the exponent polynomial order. This differs from the situation sometimes encountered with fits to Dunham-type level-energy expansions, where higher-order polynomials can sometimes follow non-physical irregularities in the data to give artificially low $\overline{dd}$ values. The results in table 1 also show that for a given overall polynomial order N_L, $\overline{dd}$ generally increases with p; this is to be expected, since the range of r for which $y_p(r)$ is relatively flat increases with p (see figure 1). Finally, we see that for a given value of p, higher-order exponent polynomials are required to achieve convergence for MLR potentials than for MLJ potentials. This is also to be expected, because the former incorporates an additional constraint.

For the MLJ_p form, potentials with $p=2$, 3 and 4 fully account for all of the data within the experimental uncertainties for overall exponent polynomial orders of $N_L \geq 6$, 7 and 7, respectively. In particular, for the $MLJ_2(4;6)$ case, the resulting total of 10 fitting parameters is much smaller (by factors of 2.4 and 4.5, respectively) than the numbers of parameters associated with the polynomial and SPW potentials of [53]. Moreover, the residuals for the 43 transitions associated with the highest observed levels $v'' = 35$–38 yield $\overline{dd}_{35} = 0.92$ for that case, a value quite similar to the analogous average dimensionless

†We are grateful to Dr Asen Pashov for providing us with these data.

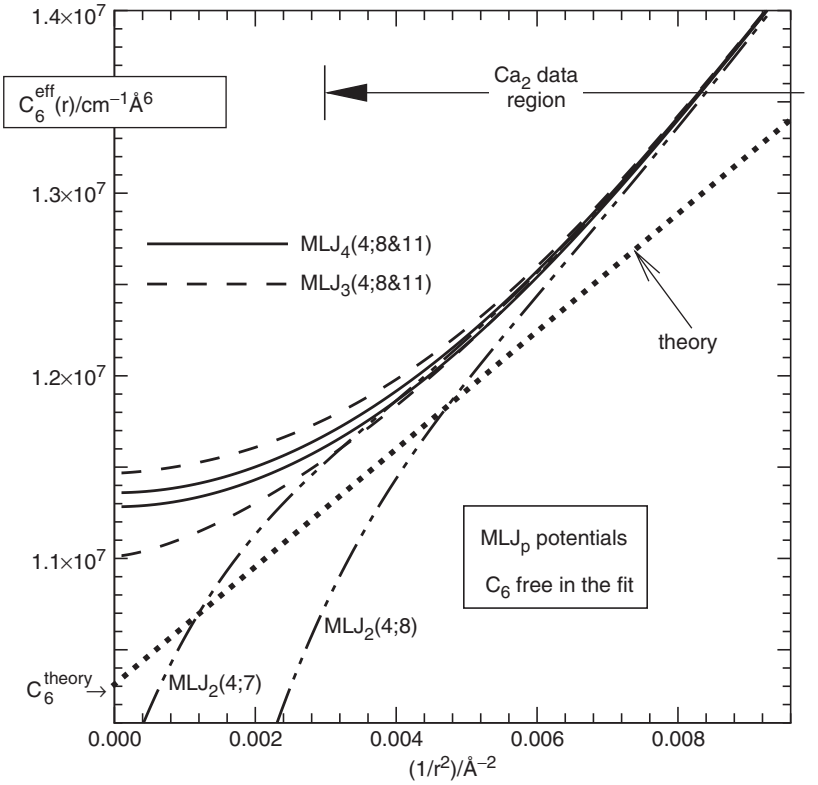

Figure 2. Long-range behaviour of MLJ_p potentials for Ca_2 determined with C_6 a free fitting parameter.

discrepancies (0.89 and 0.94) for transitions into levels $v \geq 35$ reported for the polynomial and SPW potentials of [53].

Unfortunately, although these very compact MLJ_p models both represent the data well and have the correct limiting inverse-power long-range functional form, they do not approach that limiting behaviour in the correct manner, and excessive model-dependence of the fitted values suggests that a reliable estimate of C_6 cannot be determined using this type of model. To illustrate this point, consider the behaviour of the quantity $C_6^{\text{eff}}(r)$, which is defined by a model in which the entire potential is represented by a single inverse-power term with a variable coefficient:

$$V(r) = \mathfrak{D}_e - C_6^{\text{eff}}(r)/r^6. \tag{18}$$

Theory tells us that at large r the potential function for ground-state Ca_2 takes on the form given by equation (17) [26, 27], so at long range we expect that

$$C_6^{\text{eff}}(r) \equiv r^6[\mathfrak{D}_e - V(r)] = C_6 + \frac{C_8}{r^2} + \frac{C_{10}}{r^4} + \cdots. \tag{19}$$

As a result, as $1/r^2 \to 0$ (or $r \to \infty$), $C_6^{\text{eff}}(r)$ should approach an intercept of C_6 with a slope of C_8. Moreover, theory tells us that C_6, C_8 and C_{10} coefficients are all positive for pairs of interacting ground-state atoms [23, 24]. Hence, plots of this type should approach the $1/r^2 = 0$ intercept with finite positive slope (equal to the C_8 value) and positive (upward) curvature defined by the C_{10} coefficient.

Figure 2 presents plots of $C_6^{\text{eff}}(r)$ versus $1/r^2$ for representative MLJ_p potentials; the analogous curve for the fitted $MLJ_2(4;6)$ potential would lie between those for $MLJ_2(4;7)$ and $MLJ_2(4;8)$, while the $p = 3$ and 4 potentials for $N_L = 7$, 9 and 10 lie between the corresponding curves for $N_L = 8$ and 11. This plots lead to the following conclusions.

(a) Although they are linear at the intercept, the curves for the MLJ_2 potentials have negative curvature there, not the expected positive curvature, and their limiting slopes are very much larger than C_8^{theory} [63]. This unphysical behaviour shows that these MLJ_2 potentials do not extrapolate properly.

(b) The fitted MLJ_3 and MLJ_4 potentials approach their intercepts with zero slope (see also discussion following equation (14)) rather than a positive slope

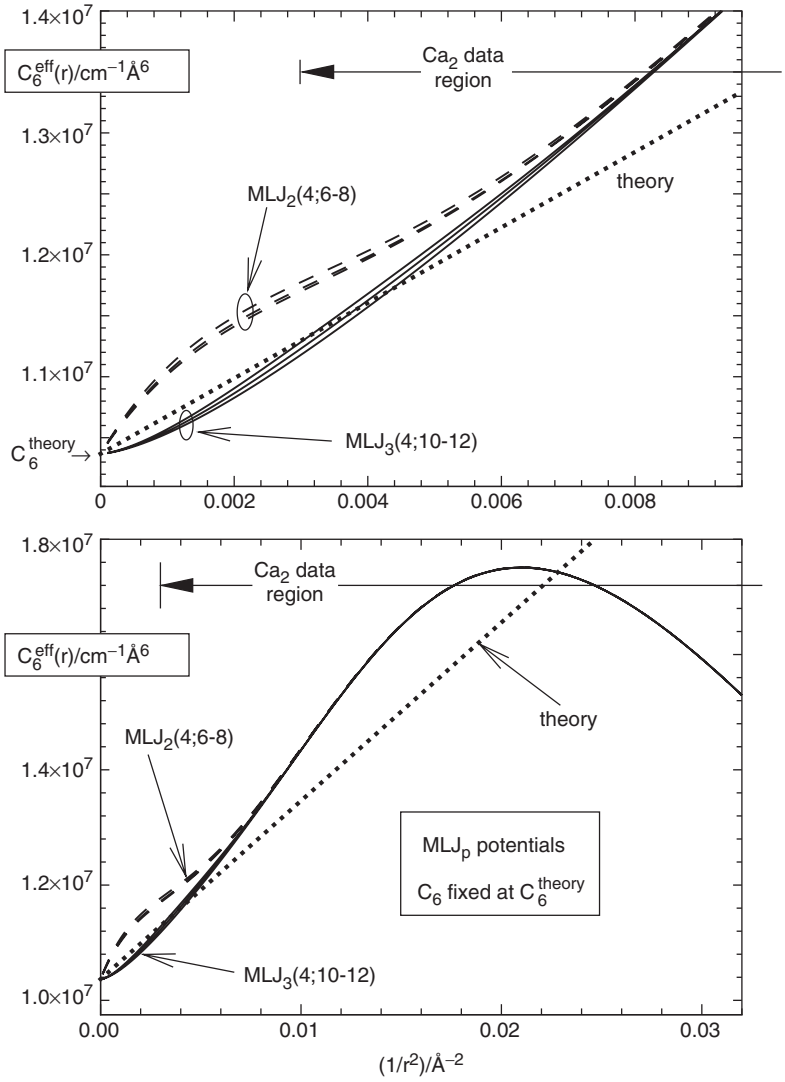

Figure 3. Long-range behaviour of MLJ_p potentials for Ca_2 determined while fixing $C_6 = C_6^{\text{theory}}$.

of magnitude comparable to the theoretical C_8 value (heavy dotted line).

(c) The intercepts of all of these MLJ potentials differ very substantially from the recent theoretical value [64] of $C_6 = 1.0368 \times 10^7 \text{cm}^{-1}\,\text{Å}^6$ (intercept of dotted line).

(d) The wide range of the C_6 value intercepts (varying from 1.15×10^7 to $0.61 \times 10^7\,\text{cm}^{-1}\,\text{Å}^6$) associated with the curves in figure 2 shows that fits to this type of model, with no constraint on the form of the leading deviation from the limiting C_6/r^6 potential function behaviour, do not yield a reliable estimate of the C_6 coefficient.

As a further test of this type of model potential, figure 3 presents plots of $C_6^{\text{eff}}(r)$ versus $1/r^2$ for representative MLJ_p potentials obtained from fits in which C_6 was held fixed at the theoretical values of Moszynski *et al.* [64]. For the cases shown, the associated fits also fully represent the data ($\overline{dd} \lesssim 0.64$), and the behaviour in the extrapolation region is much less model dependent than that seen in figure 2. However, the limiting negative curvature of the curves for the fitted $p = 2$ potentials and the fact that the $p = 3$ curves have zero slope at the intercept make their extrapolation physically incorrect.

In summary, the MLJ_p form provides very compact (few-parameter) models which accurately represent the Ca_2 data. However, when C_6 is treated as a free parameter in the fits, the extrapolation behaviour of the resulting potentials is quite unreliable, and even when C_6 is fixed at the recommended theoretical value

[64], the extrapolation behaviour has significant shortcomings. Moreover, although the $p=2$ and $p=3$ curves on figure 3 bracket the expected limiting slope, those deficiencies will not be removed by setting p at a non-integer value between 2 and 3, since the analytic form of equation (14) shows that for *any* value of p which is greater than zero, the limiting slope on the type of plot seen in figure 3 is necessarily zero. Thus, fits to MLJ_p functions are unable to yield a satisfactory description of this system.

The lower segment of table 1 summarizes the results of fits to MLR_p potentials performed with C_6 free, but with $Q_{8,6}$ fixed at the (rounded) theoretical value [63, 65] $C_8/C_6 = 30(\pm 3)\,\text{Å}^2$. They show that for $p=3$, 4 and 5, potentials expressed in terms of exponent polynomials of orders $N_L \geq 7$, 10 and 10, respectively, fully account for all of the data within the experimental uncertainties. The long-range extrapolation behaviour of these potentials is illustrated in figure 4 by plots of $C_6^{\mathrm{eff}}(r)$ for the three lowest-order 'good' fits associated with each of these values of p. As mentioned above, the attractive C_{10}/r^{10} contribution to the potential should cause the leading deviation from the limiting linear behaviour imposed on these plots by the theoretical C_8 value (slope of heavy dotted line) to be positive (upward) curvature. However, for the MLR_3 potentials this initial curvature is negative (downward). This non-physical behaviour indicates that these $p=3$ potentials are too 'floppy' to define the potential properly in the long-range region, so they are not considered further. The fact that the limiting behaviour of these $p=3$ curves is unsatisfactory is also consistent with the suggestion made earlier that the value of p should be chosen so that $(n+p)$ should be no smaller than the power of the third-longest-range term in the intermolecular potential, which in this case implies that we should choose $p \geq 4$.

For MLR_4 and MLR_5 potentials with $N_L = 10$–13 which were obtained while fixing $Q_{8,6} = 30\,\text{Å}^2$, table 2 lists the fitted values of $\mathfrak{D}_e$ and C_6, together with the values of the dimensionless RMS deviations for the overall fit, $\overline{dd}_{\mathrm{tot}}$. The last line of the table then presents averages of the individual $\mathfrak{D}_e$ and C_6 values, with overall uncertainties which take account of both the dispersion among the individual values and the individual parameter uncertainties. An additional source of uncertainty is associated with our choice of the fixed value assumed for the ratio $Q_{8,6} = C_8/C_6 = 30.0\,\text{Å}^2$ [63]. Allowing for a $\pm 10\%$ uncertainty in this quantity [65] gives rise to a 1.5% uncertainty in C_6, and $\pm 0.004\,\mathrm{cm}^{-1}$ in $\mathfrak{D}_e$; for C_6 this is the dominant contribution to the overall parameter uncertainty shown at the bottom of table 2. A noteworthy feature of the MLR_4 and MLR_5 plots

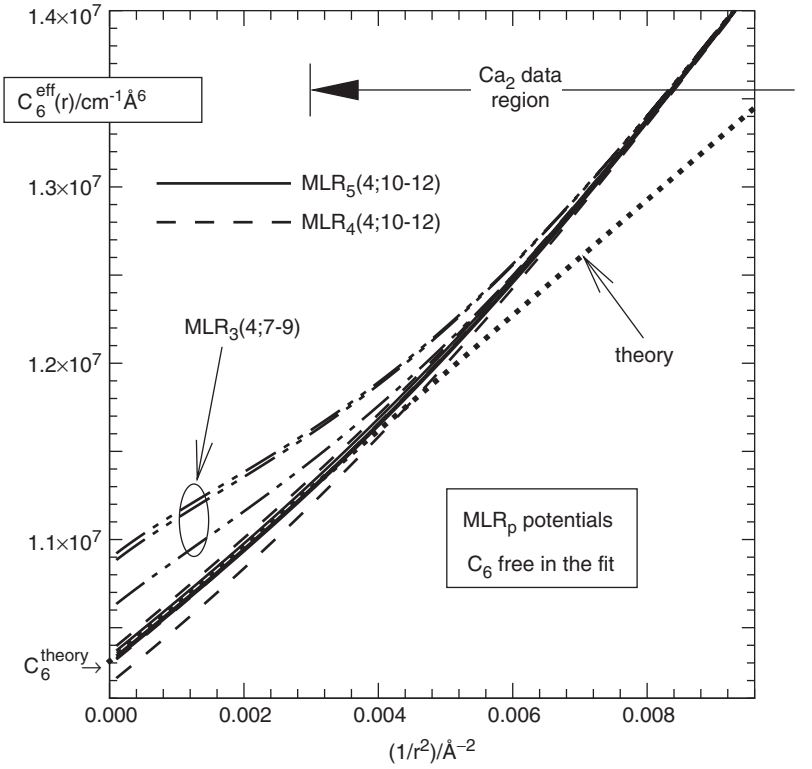

Figure 4. Long-range behaviour of MLR_p potentials for Ca_2 determined with C_6 a free fitting parameter but $Q_{8,6}$ held fixed at the theoretical value of $C_8/C_6 = 30\,\text{Å}^2$ [63].

Table 2. Results of fits to various MLR potentials performed with $Q_{8,6}$ fixed at the theoretical value $C_8/C_6 = 30.0\,\text{Å}^2$ [63]. Quantities in parentheses are 95% confidence limit uncertainties in the last digits shown, while the uncertainties in square brackets were estimated as outlined in the text.

p	$N_S; N_L$	$\overline{dd}_{\text{tot}}$	$\mathfrak{D}_e/\text{cm}^{-1}$	$C_6/10^7\,\text{cm}^{-1}\,\text{Å}^6$
4	4; 10	0.642	1102.0650 (42)	1.0193 (26)
4	4; 11	0.636	1102.0758 (49)	1.0299 (37)
4	4; 12	0.634	1102.0782 (50)	1.0375 (51)
4	4; 13	0.633	1102.0829 (60)	1.0443 (70)
5	4; 10	0.647	1102.0829 (35)	1.0348 (7)
5	4; 11	0.637	1102.0729 (40)	1.0319 (9)
5	4; 12	0.636	1102.0726 (40)	1.0306 (11)
5	4; 13	0.635	1102.0746 (43)	1.0315 (14)
	Average		1102.076 [±0.008]	1.032 [±0.02]

Table 3. Results of fits to MLR_p potentials performed with both C_6 and $Q_{8,6=C_8/C_6}$ treated as free parameters. Quantities in parentheses are 95% confidence limit uncertainties in the last digits shown.

p	$N_S; N_L$	$\overline{dd}_{\text{tot}}$	$\mathfrak{D}_e/\text{cm}^{-1}$	$C_6/10^7\,\text{cm}^{-1}\,\text{Å}^6$	$R_{8,6}\,\text{Å}^2$
4	4; 7	0.637	1102.0870 (52)	1.1260 (100)	0.8 (20)
4	4; 11	0.635	1102.0893 (87)	1.1185 (480)	4.7 (130)
4	4; 12	0.634	1102.0830 (100)	1.0705 (630)	19.8 (190)
4	4; 13	0.633	1102.0756 (110)	0.9803 (820)	52.3 (300)
5	4; 10	0.643	1102.0699 (53)	1.0095 (78)	34.7 (15)
5	4; 11	0.637	1102.0745 (54)	1.0367 (100)	29.1 (20)
5	4; 12	0.634	1102.0841 (62)	1.0622 (130)	23.8 (25)
5	4; 13	0.633	1102.0854 (66)	1.0696 (170)	22.3 (34)
Averages for $p = 5$			1102.078 [±0.009]	1.045 [±0.026]	27.5 [±5.6]

in figure 4 (solid and dashed curves) is the very small degree of model dependence in the extrapolation to the intercept; in particular, the plots for the three $p = 5$ potentials and the $\text{MLR}_4(4;11)$ potential are virtually superimposed. This gives us confidence in the physical significance of this predicted extrapolation behaviour.

Table 3 summarizes the results of fits to MLR potentials which were performed with the ratio $Q_{8,6} = C_8/C_6$ also being treated as a free fitting parameter. It shows that fits of excellent quality are obtained with exponent polynomial orders $N_L \geq 7$ and $N_L \geq 10$ for $p = 4$ and 5, respectively†. However, comparison of results for otherwise equivalent models in tables 2 and 3 shows that the quality of fit only improves marginally when $Q_{8,6}$ is also treated as a free parameter. Moreover, the large relative uncertainties and high degree of model dependence of the $Q_{8,6}$ values associated with the $p = 4$ MLR potentials indicates that fits to the MLR_4 potential form cannot provide a reliable experimental estimate of this quantity. On the other hand, the results for the various MLR_5 potentials show much less model dependence, and in the absence of other information, those average values would define our best estimates of these quantities.

4.3. *Optimal estimates of the potential function and its long-range properties*

The Ca_2 data analysis presented above had two main objectives: the first was to demonstrate the utility of the two-term MLR potential function form, and to ascertain how accurately it can determine a molecule's dissociation energy and long-range potential coefficients in the absence of other information. The results in the last three columns of table 4 show that the present values of the three parameters defining the potential function tail agree with those of the most recent analysis of Allard

†Results for MLR_4 potentials with $N_L = 8 - 10$ are omitted because those fits attempted to converge on unphysical negative values of $Q_{8,6}$.

Table 4. Comparison with parameters obtained in previous work.

	Present			
	Recommended	Fitted freely	Allard *et al.* [53]	Theory
$\mathfrak{D}_e/cm^{-1}$	1102.076 [±0.008]	1102.078 [±0.009]	1102.060 or 1102.074	1113[a]
$\mathfrak{D}_0/cm^{-1}$	1069.869 [±0.009][b]	1069.872 [±0.011][b]	1069.868 [±0.010][b]	
$C_6/10^7 cm^{-1}$ Å^6	1.032 [±0.02]	1.045 [±0.026]	1.003 [±0.033]	1.0366[c]
$(C_8/C_6)/Å^2$	[30.0][d]	27.5 [±5.6]	31.4–44.5	29.85 [±3.0][e]

[a]See [63]. This value is not expected to be particularly accurate.
[b]Defined as the binding energy of the zero point level.
[c]From [64].
[d]Fixed (rounded) theoretical value [63].
[e]From [63] and [65].

et al. [53] and with the best current theoretical values well within the uncertainties. Moreover, the values of C_6 and C_8/C_6 obtained herein are distinctly closer to the current best *ab initio* values than are those of Allard *et al*. [53]. Unfortunately, the uncertainties associated with the present empirical determination of the ratio C_8/C_6 are still relatively large, and inter-parameter correlation means that this leads to an empirically determined C_6 value with an uncertainty which is somewhat higher than might be necessary.

The second objective of our Ca_2 analysis was to determine the best possible empirical estimates of the dissociation energy and long-range potential coefficient(s) of this state. The approach taken here is based on the intuitive assumption that in *ab initio* calculations of C_6 and C_8 at a given level of theory, the ratio of the resulting coefficients will tend to be more accurate than the individual values. The estimate for the uncertainty in the theoretical C_8/C_6 ratio given above was based on an estimate [65] of 10% for the uncertainty in the calculated C_8 coefficient [63]. However, we note that the values of this ratio defined by the theoretical long-range potential coefficients reported in [63] and [66] (29.85 and 27.33 Å^2, respectively) agree to within 6.9%, although the associated C_6 coefficients differ by up to 13.6%. Similarly, the values of this quantity yielded by the relativistic and non-relativistic calculations of [63] (29.85 and 29.74 Å^2, respectively) differ by only 0.37%, while the associated C_6 coefficients differ by 1.9%. Thus, it seems reasonable to conclude that the true uncertainty in the (rounded) theoretical value of $C_8/C_6 = 30$ Å^2 is somewhat smaller than 10%, and that it is considerably smaller than the uncertainty in our empirical value of 27.5(±5.6) Å^2.

The above considerations led us to conclude that the best possible empirical values of $\mathfrak{D}_e$ and C_6 for this system would be those obtained from fits performed while fixing $C_8/C_6 = 30$ Å^2, as summarized in the last row of table 2 and first column of table 4. These values are incorporated in our final recommended potential energy function model, the $MLR_5(4;11)$ function whose parameters are listed in table 5. The numbers of digits required to represent its exponent expansion parameters were minimized using the sequential rounding and refitting procedure of [67]. Uncertainties are not listed for the individual ϕ_i values since they have no distinct physical significance, while those associated with the physically interesting parameters $\mathfrak{D}_e$ and C_6 are estimates based on the model dependence illustrated by table 2, on the uncertainties associated with the individual fits, and on the effect of the estimated uncertainty in the value of $Q_{8,6}$ obtained from theory.

Table 5. Parameters defining our recommended $MLR_5(4;11)$ potential energy function for the $X^1\Sigma_g^+$ state of Ca_2. This fit to this model yields $\overline{dd}_{tot} = 0.637$ and $\overline{dd}_{35} = 0.91$.

$\mathfrak{D}_e/cm^{-1}$	1102.076 [±0.008]
$\mathfrak{D}_0/cm^{-1}$	1069.870 [±0.009]
C_6/cm^{-1} Å^6	1.032 [±0.02] × 10^7
$C_8/C_6/Å^2$	30
$r_e/Å$	4.27781 [±0.00003]
ϕ_0	−1.074136
ϕ_1	0.0232
ϕ_2	−0.42734
ϕ_3	−0.1602
ϕ_4	−0.3443
ϕ_5	−8.228
ϕ_6	72.177
ϕ_7	−291.79
ϕ_8	639.5
ϕ_9	−797.5
ϕ_{10}	533
ϕ_{11}	−150

5. Discussion and conclusions

The present work shows that the new MLR potential form can provide an accurate representation of the

extensive high resolution Ca_2 data of Allard *et al.* [52, 53], which is much more compact and than previously reported potentials [53] based on this same data set. In particular, the polynomial potential of [53] is defined in terms of 21 polynomial coefficients (each specified to 18 significant digits!), two long-range fitting parameters, plus three other parameters chosen to give '... good convergence of the fitting procedure', for a total of 26. The alternate SPW form used by Allard *et al.* [53] is defined by a grid of 48 points, the energy of each being a free parameter, plus three additional fitting parameters associated with the analytic inverse-power tail. In contrast, the present potential is defined in terms of a mere 15 fitting parameters plus one manually chosen parameter, $p = 5$, and one fixed long-range parameter ($Q_{8,6}$), for a total of 17, and no separate potential segments need to be attached at short or long range. The fact that the present potential is a single compact analytic function will also make it relatively easy to use.

It is also interesting to see that, although the difference is within the estimated uncertainties, our recommended experimental value of C_6 for this system is distinctly closer to the recent theoretical value of Moszynski *et al.* [64] than is the value reported by Allard *et al.* [53]. Moreover, our estimated uncertainty in C_6 is based on an estimated 10% uncertainty for the theoretical C_8/C_6 value which discussion above suggests is somewhat pessimistic, and may have made our estimates of the uncertainties in our recommended empirical $\mathfrak{D}_e$ and C_6 values (first column in table 4) somewhat pessimistic.

In spite of the differences noted above, it is important to remember that the polynomial and SPW potentials of Allard *et al.* [53] do provide an equally good representation of the Ca_2 data, and table 4 shows that their estimates of the dissociation energy and long-range potential coefficients are quite close, both to the values obtained here and to the current best theoretical values. This clearly affirms the validity and reliability of all three approaches. Moreover, the SPW potential form would probably be the 'method of choice' for treating cases in which the potential function undergoes abrupt changes in shape or other types of irregular behaviour. However, the more compact (fewer parameters being required) unified form of the MLR potential make it easier to use, and will make it a particularly convenient choice for future work.

Three cautionary notes raised by the present study concern the ability of DPF analyses to determine reliable estimates of dissociation limits and long-range potential coefficients. In particular, the discussion associated with figures 2 and 3 suggests that a potential model which incorporates only a single long-range inverse-power term (such as the MLJ potential) may not provide a realistic extrapolation beyond the data region, even if the experimental data extend almost all the way to dissociation, unless a good estimate of the limiting C_n potential coefficient is available and is held fixed in the fit. Fortunately, this has been the case in almost all applications of the MLJ potential function form reported to date [30–33, 35, 37–44]. The second point is that the determination of a reliable estimate of the limiting long-range potential coefficient C_n (C_6 in the present work) by a DPF analysis using the MLR form may not be possible unless some plausible estimate of the relative strength of the second term in the long-range potential is known and held constant in the fit, in order to constrain the leading deviation from the limiting behaviour of equation (8) to have the correct qualitative form. Finally, this study illustrates the more general point that model dependence is often the dominant source of uncertainty affecting the determination of physically interesting quantities from experimental data.

While the present application of the MLR form was based on the simple two-term $u_{LR}(r)$ of equation (11), it would be straightforward to generalize it to incorporate three or more specified inverse-power terms in the long-range tail, as in

$$u_{LR}(r) = \frac{C_n}{r^n} + \frac{C_{m_1}}{r^{m_1}} + \frac{C_{m_2}}{r^{m_2}} = \frac{C_n}{r^n}\left[1 + \frac{Q_{m_1,n}}{r^{m_1-n}} + \frac{Q_{m_2,n}}{r^{m_2-n}}\right] \tag{20}$$

or to incorporate damping functions [45–47] into each of the inverse-power terms. It should also be possible to utilize more complicated expressions for $u_{LR}(r)$ which take account of inter-state coupling [68, 69]. However, the discussion associated with equation (14) places some practical limits on such extensions of the model, in that the power p defining the radial expansion variable $y_p(r)$ must be larger than the difference between the largest and smallest powers of the inverse-power terms contributing to $u_{LR}(r)$, $p > (m_{max} - n)$. As shown by figure 1, the domain of r/r_e over which $|y_p(r)|$ differs significantly from unity becomes ever narrower with increasing values of p, so for large values of $(m_{max} - n)$ the exponent coefficient $\phi(r)$ will have limited region of flexibility. However, a more practical limitation may prove to be the availability of realistic theoretical estimates for the long-range potential coefficient ratios $Q_{m_j,n}$ to utilize in such expressions. In any case, some of these extended versions of the MLR form will be examined in future work.

The MLR potential function form has been used in one previous DPF analysis, in a case in which the experimental data spanned only half the potential

well [35]. As a result, that analysis could not have been expected to determine $\mathfrak{D}_e$ or the long-range potential coefficients. However, it was shown there that imposition of the two-term limiting long-range MLR behaviour of equation (12) with both C_6 and $Q_{8,6}$ fixed at theoretical values, ensured that the resulting potential would provide particularly realistic extrapolation behaviour in the interval from the data region to the asymptote. The present application to Ca_2 is a much more challenging case, since the fact that the data being treated span 99.97% of the potential well places much more severe demands on the flexibility of this functional form. Its success in representing the data in a much more compact manner than was done in previous work with the same data set attests to its utility.

Acknowledgement

We are pleased to acknowledge stimulating discussions with Dr A. J. Ross which have helped expand our understanding of the nature and utility of the MLR form. This research was supported by the Natural Sciences and Engineering Research Council of Canada through a Discovery Grant to RJL and a Summer Research Award to RDEH.

References

[1] R. Rydberg, Z. Phys. **73,** 376 (1931); O. Klein, Z. Phys. **76,** 226 (1932); R. Rydberg, Z. Phys. **80,** 514 (1933); A. L. G. Rees, Proc. Phys. Soc. (London) **59,** 998 (1947).
[2] R. J. Le Roy and W.-H. Lam, Chem. Phys. Lett. **71,** 544 (1980).
[3] J. Tellinghuisen, J. Chem. Phys. **78,** 2374 (1983).
[4] J. W. Tromp and R. J. Le Roy, J. Molec. Spectrosc. **109,** 352 (1985).
[5] K. J. Jordan, R. H. Lipson, N. A. McDonald, and R. J. Le Roy, J. Phys. Chem. **96,** 4778 (1992).
[6] R. J. Le Roy, J. Chem. Phys. **101,** 10217 (1994).
[7] D. R. T. Appadoo, R. J. Le Roy, P. F. Bernath, S. Gerstenkorn, P. Luc, J. Vergès, J. Sinzelle, J. Chevillard, and Y. D'Aignaux, J. Chem. Phys. **104,** 903 (1996).
[8] J. K. G. Watson, J. Molec. Spectrosc. **80,** 411 (1980).
[9] J. K. G. Watson, J. Molec. Spectrosc. **223,** 39 (2004).
[10] R. J. Le Roy and Y. Huang, J. Molec. Struct. (Theochem) **591,** 175 (2002).
[11] R. J. Le Roy, J. Seto, and Y. Huang, DPotFit 1.1: a computer program for fitting diatomic molecule spectra to potential energy functions, University of Waterloo Chemical Physics Research Report CP-662R (University of Waterloo, 2006); see http://leroy.uwaterloo.ca/programs/.
[12] J. A. Coxon and P. G. Hajigeorgiou, J. Molec. Spectrosc. **150,** 1 (1991).
[13] J. A. Coxon and P. G. Hajigeorgiou, Can. J. Phys. **94,** 40 (1992).
[14] J. A. Coxon, J. Molec. Spectrosc. **152,** 274 (1992).
[15] J. A. Coxon and P. G. Hajigeorgiou, Chem. Phys. **167,** 327 (1992).
[16] H. G. Hedderich, M. Dulick, and P. F. Bernath, J. Chem. Phys. **99,** 8363 (1993).
[17] J. B. White, M. Dulick, and P. F. Bernath, J. Chem. Phys. **99,** 8371 (1993).
[18] J. M. Campbell, M. Dulick, D. Klapstein, J. B. White, and P. F. Bernath, J. Chem. Phys. **99,** 8379 (1993).
[19] E. G. Lee, J. Y. Seto, T. Hirao, P. F. Bernath, and R. J. Le Roy, J. Molec. Spectrosc. **194,** 197 (1999).
[20] J. Y. Seto, Z. Morbi, F. Charron, S. K. Lee, P. F. Bernath, and R. J. Le Roy, J. Chem. Phys. **110,** 11756 (1999).
[21] R. J. Le Roy, D. R. T. Appadoo. K. Anderson, A. Shayesteh. I. E. Gordon, and P. F. Bernath, J. Chem. Phys. **123,** 204304:1 (2005).
[22] H. Margenau, Rev. Mod. Phys. **11,** 1 (1939).
[23] J. O. Hirschfelder, C. F. Curtiss, and R. B. Bird, *Molecular Theory of Gases and Liquids* (Wiley, New York, 1964).
[24] J. O. Hirschfelder and W. J. Meath, in *Intermolecular Forces*, Vol. 12, in the series *Advances in Chemical Physics*, edited by J. O. Hirschfelder (Interscience, New York, 1967), Chap. 1, pp. 3–106.
[25] W. J. Meath, Am. J. Phys. **40,** 21 (1972).
[26] R. J. Le Roy and R. B. Bernstein, J. Chem. Phys. **52,** 3869 (1970).
[27] R. J. Le Roy, in *Molecular Spectroscopy*, edited by R. Barrow, D. A. Long, and D. J. Millen (Chemical Society of London, London, 1973), Vol. 1, Specialist Periodical Report 3, pp. 113–176.
[28] P. G. Hajigeorgiou and R. J. Le Roy, in 49th Ohio State University International Symposium on Molecular Spectroscopy, Columbus, Ohio, June 13–17, 1994, paper WE04.
[29] P. G. Hajigeorgiou and R. J. Le Roy, J. Chem. Phys. **112,** 3949 (2000).
[30] J. A. Coxon and R. Colin, J. Molec. Spectrosc. **181,** 215 (1997).
[31] J. A. Coxon and P. G. Hajigeorgiou, J. Molec. Spectrosc. **193,** 306 (1999).
[32] J. Y. Seto, R. J. Le Roy, J. Vergès, and C. Amiot, J. Chem. Phys. **113,** 3067 (2000).
[33] J. A. Coxon and P. G. Hajigeorgiou, J. Molec. Spectrosc. **203,** 49 (2000).
[34] Y. Huang, Determining analytical potential energy functions of diatomic molecules by direct fitting. MSc thesis, Department of Chemistry, University of Waterloo (2001).
[35] R. J. Le Roy, Y. Huang, and C. Jary, J. Chem. Phys. **125,** 164310 (2006).
[36] Y. Huang and R. J. Le Roy, J. Chem. Phys. **119,** 7398 (2003).
[37] J.-U. Grabow, A. S. Pine, G. T. Fraser, F. J. Lovas, and R. D. Suenram, J. Chem. Phys. **102,** 1181 (1995).
[38] T. C. Melville, C. Linton, and J. A. Coxon, J. Molec. Spectrosc. **204,** 291 (2000).
[39] T. C. Melville and J. A. Coxon, Spectrochim. Acta A **57,** 1171 (2001).
[40] O. Docenko, O. Nikolayeva, M. Tamanis, R. Ferber, E. A. Pazyuk, and A. V. Stolyarov, Phys. Rev. A **66,** 052508 (2002).
[41] J. A. Coxon and P. G. Hajigeorgiou, J. Chem. Phys. **121,** 2992 (2004).

[42] J. A. Coxon and C. S. Dickinson, J. Chem. Phys. **121,** 9378 (2004).
[43] J. A. Coxon and T. C. Melville, J. Molec. Spectrosc. **235,** 235 (2006).
[44] J. A. Coxon and P. G. Hajigeorgiou, J. Phys. Chem. **A110**, 6261 (2006).
[45] A. Koide, W. J. Meath, and A. R. Allnatt, Chem. Phys. **58,** 105 (1981).
[46] C. Douketis, G. Scoles, S. Marchetti, M. Zen, and A. J. Thakkar, J. Chem. Phys. **76,** 3057 (1982).
[47] K. T. Tang and J. P. Toennies, J. Chem. Phys. **80,** 3726 (1984).
[48] H. Kreek and W. J. Meath, J. Chem. Phys. **50,** 2289 (1969).
[49] H. Kreek, Y. H. Pan, and W. J. Meath, Molec. Phys. **19,** 513 (1970).
[50] R. J. Le Roy, DParFit 3.3: a computer program for fitting multi-isotopologue diatomic molecule spectra, University of Waterloo Chemical Physics Research Report CP-660 (University of Waterloo, 2005); see http://leroy.uwaterloo.ca/programs/.
[51] R. J. Le Roy, phiFIT 1.1: a computer program to fit potential function points to selected analytic functions, University of Waterloo Chemical Physics Research Report CP-663R (University of Waterloo, 2006); see http://leroy.uwaterloo.ca/programs/.
[52] O. Allard, A. Pashov, H. Knöckel, and E. Tiemann, Phys. Rev. A **66,** 042503 (2002).
[53] O. Allard, C. Samuelis, A. Pashov, H. Knöckel, and E. Tiemann, Eur. Phys. J. D **26,** 155 (2003).
[54] E. Tiemann, Z. Phys. D At. Molec. Clusters **5,** 77 (1987).
[55] U. Wolf and E. Tiemann, Chem. Phys. Lett. **133,** 116 (1987).
[56] U. Wolf and E. Tiemann, Chem. Phys. Lett. **139,** 191 (1987).
[57] U. Wolf and E. Tiemann, Chem. Phys. **119,** 407 (1988).
[58] E. Tiemann, Molec. Phys. **65,** 359 (1988).
[59] A. Pashov, W. Jastrzębski, and P. Kowalczyk, Comp. Phys. Comm. **128,** 622 (2000).
[60] A. Pashov, W. Jastrzębski, and P. Kowalczyk, J. Chem. Phys. **113,** 6624 (2000).
[61] A. Pashov, W. Jastrzębski, W. Jaśniecki, V. Bednarska, and P. Kowalczyk, J. Molec. Spectrosc. **203,** 264 (2000).
[62] S. G. Porsev and A. Derevianko, Phys. Rev. A **65,** 020701 (2002).
[63] B. Bussery-Honvault, J.-M. Launay, and R. Moszynski, Phys. Rev. A **68,** 032718 (2003).
[64] R. Moszynski, G. Lach, M. Jaszuński, and B. Bussery-Honvault, Phys. Rev. A **68,** 052706 (2003).
[65] R. Moszynski, private communication (2006).
[66] F. Maeder and W. Kutzelnigg, Chem. Phys. **42,** 94 (1979).
[67] R. J. Le Roy, J. Molec. Spectrosc. **191,** 223 (1998).
[68] F. Martin, M. Aubert-Frécon, R. Bacis, P. Crozet, C. Linton, S. Magnier, A. J. Ross, and I. Russier, Phys. Rev. A **55,** 3458 (1997).
[69] M. Aubert-Frécon, S. Rousseau, G. Hadinger, and S. Magnier, J. Molec. Spectrosc. **192,** 239 (1998).